ACS APPLIED MATERIALS & INTERFACES

Spotlight on Applications

www.acsami.org

Atomic Oxygen Effects on POSS Polyimides in Low Earth Orbit

Timothy K. Minton,*[,†] Michael E. Wright,*[,⊥] Sandra J. Tomczak,*[,‡] Sara A. Marquez,[†] Linhan Shen,[†] Amy L. Brunsvold,[†] Russell Cooper,[†] Jianming Zhang,[†] Vandana Vij,[§] Andrew J. Guenthner,[#] and Brian J. Petteys[⊥]

[†]Department of Chemistry and Biochemistry, Montana State University, 103 Chem/Biochem Building, Bozeman, Montana 59717, United States

[‡]AFRL/RZSB, Motor Branch, Air Force Research Laboratory, 4 Draco Drive, Building 8351, Edwards AFB, Calfornia 93524, United States

[§]ERC Incorporated, Materials Applications Branch, Air Force Research Laboratory, 10 E. Saturn Boulevard, Building 8451, Edwards AFB, Califronia 93524, United States

[⊥]Research and Engineering Sciences Department, Chemistry Division, NAVAIR-US NAVY, China Lake, California 93555, United States

[#]AFRL/RZSM, Materials Applications Branch, Air Force Research Laboratory, 10 E. Saturn Boulevard, Building 8451, Edwards AFB, California 93524, United States

ABSTRACT: Kapton polyimde is extensively used in solar arrays, spacecraft thermal blankets, and space inflatable structures. Upon exposure to atomic oxygen in low Earth orbit (LEO), Kapton is severely eroded. An effective approach to prevent this erosion is to incorporate polyhedral oligomeric silsesquioxane (POSS) into the polyimide matrix by copolymerizing POSS monomers with the polyimide precursor. The copolymerization of POSS provides Si and O in the polymer matrix on the nano level. During exposure of POSS polyimide to atomic oxygen, organic material is degraded, and a silica passivation layer is formed. This silica layer protects the underlying polymer from further degradation. Laboratory and space-flight experiments have shown that POSS polyimides are highly resistant to atomic-oxygen attack, with erosion yields that may be as little as 1% those of Kapton. The results of all the studies indicate that POSS polyimide would be a space-survivable replacement for Kapton on spacecraft that operate in the LEO environment.

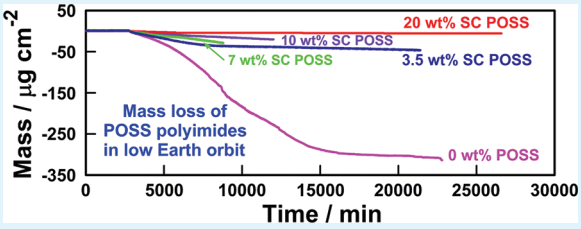

KEYWORDS: *hyperthermal atomic oxygen, polyimide, polyhedral oligomeric silsesquioxane, POSS, space environment, polymer erosion, low Earth orbit*

1. INTRODUCTION

Organic materials exposed to the low Earth orbit (LEO) environment typically erode away. Many studies have documented how polymers that can withstand decades of exposure on Earth are quickly eroded and converted to carbon dioxide and other gaseous materials within days to months during exposure in LEO.[1−9] The primary mechanism for destroying organic hydrocarbon materials is oxidation by atomic oxygen,[7,10−20] which can be more than 90% of the neutral component of the residual atmosphere at altitudes of 300−700 km.[21,22] Although in many cases organic materials could offer savings in weight, design, and manufacturing methods, all pivotal for spacecraft construction, they are not chemically stable in LEO and must be protected. Polymers are typically protected by the application of a coating, often silica-based, which is resistant to degradation in the presence of atomic oxygen.[23−29] However, imperfections in the coating created during its deposition, or by physical damage that occurs during flight, lead to erosion of the polymer substrate.[3,23,24] For this reason, alternative and self-regenerative methods of protection are sought for organic polymeric materials used in space.[30−33] Kapton polyimide is ubiquitous in space applications because of its temperature stability, insulation properties, IR transparency, resistance to UV damage, thermo-optical characteristics, and mechanical properties.[34−38] This Spotlight summarizes nearly a decade of work on the performance of Kapton-like polyimides that have been developed to be resistant to degradation by atomic oxygen. Earlier results from laboratory- and space-based studies are given, as well as new information on the synthesis and in-space performance of a recently developed polyimide.

Polyimides are known for their thermal stability, chemical solvent resistance, and mechanical properties, and they can be made using very simple chemical reactions and processing methods.[39,40] Polyimide synthesis and processing was pioneered by workers at Dupont in the 1950's, with Kapton being the first commercially significant polyimide. Polyimides

Received: October 31, 2011
Accepted: December 21, 2011
Published: December 21, 2011

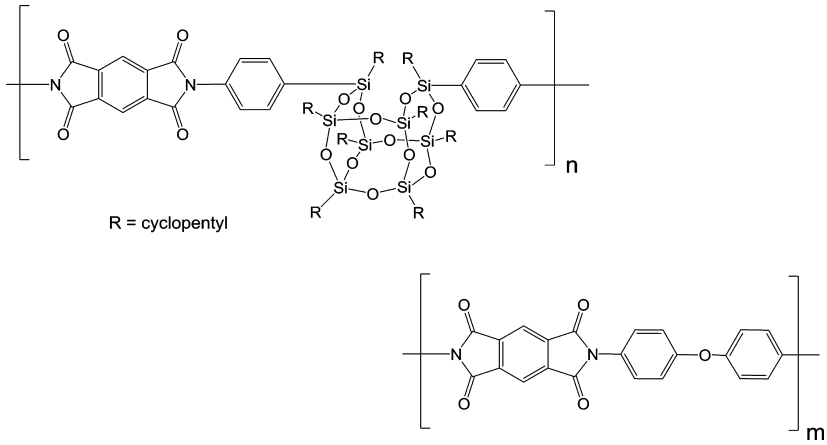

Figure 1. MC POSS polyimide structure demonstrating the PMDA-MC-POSS repeat unit and the PMDA-ODA repeat unit, where R = cyclopentyl and *n* and *m* are mole fractions that sum to one.

are generally formed in a polar solvent through the condensation of a dianhydride monomer and a diamine monomer. High-molecular-weight poly(amic acid) readily forms bythe nucleophilic attack of an amino group on an anhydride carbonyl group. The poly(amic acid) then undergoes either chemical imidization or solvent evaporation followed by thermal imidization. During imidization the poly(amic acid) forms polyimide through ring-closure and concurrent loss of water.[39,40]

We have produced durable polymers through the incorporation of polyhedral oligomeric silsesquioxane (POSS) into a Kapton-like polyimide through copolymerization of POSS diamine monomers.[41−49] POSS is a unique family of nanoscale inorganic/organic hybrid cage-like structures that contain a silicon/oxygen framework ($RSiO_{1.5}$), where R is a hydrocarbon group that can be utilized to tailor compatibility with the polymer and chemical stability (e.g. alkyl versus aryl).[43] We have demonstrated that POSS-diamines can be incorporated into the poly(amic acid) polymerization without changes to polymerization conditions or to the subsequent cure cycles. POSS units may be incorporated at significant loading levels with only modest effects on mechanical, chemical, and optical properties of the final POSS-polyimide material.[46−49] We have conducted a variety of studies of POSS polyimides by exposing their surfaces to beams of hyperthermal oxygen atoms and measuring mass loss in situ, or surface recession, morphology, and chemistry ex situ. We have also carried out similar studies of POSS polyimides that were exposed to an atomic-oxygen environment on the International Space Station. We report here the results of numerous studies, which, taken together, demonstrate the potential utility of POSS polyimides as space survivable materials that may replace Kapton. While some of us have studied thermal and mechanical properties,[46−49] and other researchers have studied the superior properties of POSS polyimides with respect to hypervelocity impacts,[50−52] the focus of this Spotlight is on the atomic-oxygen resistance of POSS polyimides and their performance in LEO.

Two POSS polyimides were studied, and they showed similar resistance to atomic-oxygen attack. In one type of POSS polyimide, the POSS monomer was incorporated into the main chain of the polymer backbone (main-chain POSS polyimide), and in the other the POSS monomer was incorporated as a pendant group on the polymer backbone (side-chain POSS polyimide). Although the main-chain POSS polyimide was developed earlier, the synthesis of the monomer for the side-chain POSS polyimide is simpler, making the side-chain POSS polyimide easier to produce.

2. EXPERIMENTAL DETAILS

2.1. Preparation of Main-Chain POSS Polyimides. A POSS dianiline monomer with two 1-(4-aminophenyl)-pendant groups and eight cyclopentyl pendant groups was first synthesized using a procedure described by Wright et al. and was used to prepare well-characterized poly(amide) oligomers.[53] Gonzalez[41] later described the preparation of POSS-containing pyromellitic dianhydride (PMDA)/oxydianiline (ODA) poly(amic acids) and the subsequent thermal curing of the poly(amic acids) into a Kapton-like POSS-polyimide film. The resulting co-polymer incorporates a POSS cage into the main chain of the polymer backbone and is thus referred to as main-chain (MC) POSS polyimide (see Figure 1). Using poly(amic acids) prepared by the method of Gonzalez, MC POSS polyimide random copolymers were synthesized with POSS monomer loadings corresponding to 0, 5, 10, 20, and 25 wt %, which correspond to Si_8O_{11} cage loadings of 0, 1.75, 3.5, 7.0, and 8.8 wt %, respectively. Free-standing polymer films were prepared as described by Gonzalez, and spin-coated films were deposited onto quartz crystal microbalance (QCM) discs as described below.

2.2. Synthesis of Side-Chain POSS Monomer. *2.2.1. General Methods.* The reaction scheme for the synthesis of the monomer for producing a side-chain (SC) POSS polyimide is shown in Figure 2. All manipulations of compounds and solvents were carried out using standard Schlenk techniques. ^1H and ^{13}C NMR measurements were performed using a Bruker AC 200 or Bruker 400 MHz instrument. ^1H and ^{13}C NMR chemical shifts are reported versus the deuterated solvent peak (Solvent, ^1H, ^{13}C: $CDCl_3$, δ 7.18 ppm, δ 77.0 ppm). 3,5-dinitrobenzoyl chloride, anhydrous THF, triethylamine (anhydrous grade), and platinum oxide were purchased from Sigma Aldrich and used as received. (aminopropyl)-hepta-isobutylPOSS was purchased from Hybrid Plastics and used as received. 4,4′-diaminodiphenyl ether (oxydianiline; ODA) (Lancaster, 98 %) was purified by recrystallization as follows: Under N_2 the ODA (5.00 g) was dissolved in N,N-dimethylformamide (25 mL, Sigma Aldrich, 99.9+ %) and placed in a 90 °C oil bath. This mixture was diluted with hot (90 °C) toluene (200 ml, J.T. Baker, 99.9+ %) and mixed thoroughly. The clear solution was stored under N_2 in the dark for 24 h and then the crystals were collected by suction filtration under N_2. The light tan ODA crystals were dried at 100 °C overnight in a vacuum oven having a low N_2 purge rate and then stored under N_2. Pyromellitic dianhydride (PMDA) was recrystallized from 90 °C 1,4-dioxane (Sigma Aldrich, 99 +%) and dried at 100 °C overnight in a vacuum oven, with a low N_2 flow, and then stored under N_2. N,N-dimethylacetamide (DMAc) (Aldrich, 99.9 + %) was distilled from BaO under reduced pressure directly onto activated molecular sieves (Davison Chemical,

dx.doi.org/10.1021/am201509n | ACS Appl. Mater. Interfaces 2012, 4, 492−502

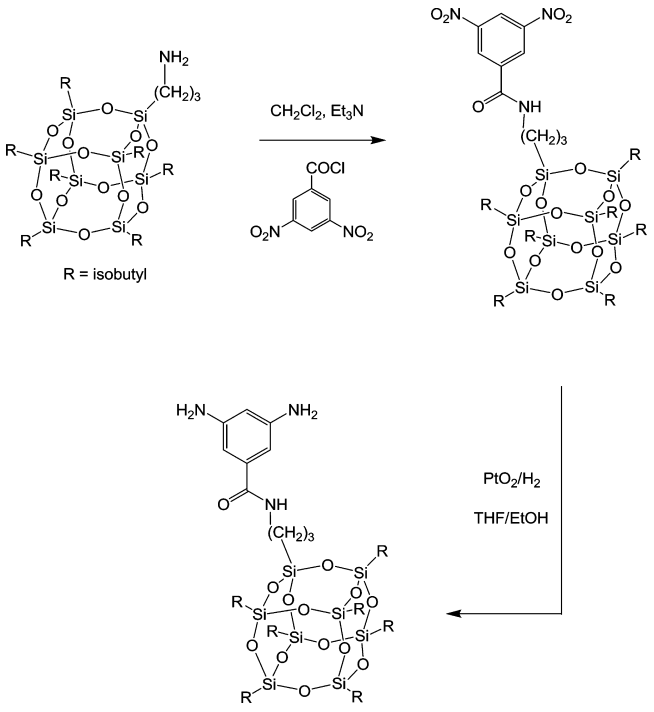

Figure 2. Reaction scheme for the synthesis of the *N*-[(hepta-isobutylPOSS)propyl]-3,5-diaminobenzamide monomer used to prepare side-chain (SC) POSS polyimide polymers.

8-12 mesh, 4 Å pore size) and then stored in a drybox. Elemental analyses were performed at Atlantic Microlab, Inc., Norcross, GA.

*2.2.2. N-{3-(R$_7$Si$_8$O$_{12}$)propyl}-3,5-diaminobenzamide [R = isobutyl] (**1**).* A CH_2Cl_2 (200 ml) solution containing 3-aminopropyl-(hepta-isobutyl)POSS (15.60 g, 17.84 mmol) and triethylamine (5 mL) was chilled to 0 °C and then treated with 3,5-dinitrobenzoyl chloride (4.34 g, 18.73 mmol). The mixture was allowed to react with stirring at 0 °C for 4 h. The mixture was diluted with water and the organic layer was separated and washed with water, sat. aq. $NaHCO_3$ (2 x 150 mL), brine (100 mL), and then dried over $MgSO_4$. The solvent was removed under reduced pressure to give *N*-[(hepta-isobutyl-POSS)propyl]-3,5-dinitrobenzamide as an off-white solid (18.8 g, 98%). ^{1}H NMR ($CDCl_3$) δ 9.16 (t, J = 2.1 Hz, 1H), 8.91 (d, J = 2.1 Hz, 2H), 6.33 (br t, 1H, NH), 3.52 (appt q, 2H), 1.95-1.69 (m, 9H), 0.96-0.93 (m, 42H), 0.65-0.55 (m, 14H); ^{13}C NMR ($CDCl_3$) δ 162.6, 148.7, 138.2, 127.0, 121.0, 43.1, 25.7, 25.4, 23.9, 23.8, 22.9, 22.5, 9.6. Anal. Calcd for $C_{38}H_{70}N_3O_{17}Si_8$: C, 42.83; H, 6.62. Found: C, 42.73; H, 6.80.

*2.2.3. N-[(Hepta-isobutylPOSS)propyl]-3,5-diaminobenzamide (**2**).* A Schlenk flask was charged with *N*-[(hepta-isobutylPOSS)-propyl]-3,5-dinitrobenzamide (18.8 g, 17.6 mmol), PtO_2 (1.00 g), THF (120 mL), and ethanol (40 mL). The reaction vessel was charged with H_2 (~2 psig, then 4 evacuation/backfill cycles) and allowed to react with stirring for 16 h. The mixture was filtered through a pad of Celite, and the solvents were removed under reduced pressure to give *N*-[(isobutyl-POSS)propyl]-3,5-diaminobenzamide as an off-white solid (17.3 g, 97%). ^{1}H NMR ($CDCl_3$): δ 6.43 (d, J = 2.0 Hz, 2H), 6.10 (t, J = 2.0 Hz, 1H), 5.96 (br t, 1H, NH), 3.66 (br s, 4H, NH_2), 3.39 (br appt q, 2H), 1.95-1.74 (appt. sept. 7H), 1.71-1.62 (m, 2H) 0.96 (br. s, 21H), 0.93 (br. s, 21H), 0.69-0.63 (m, 2H), 0.61 (d, J = 1.8 Hz, 7H), 0.57 (d, J = 1.8 Hz, 7H). ^{13}C NMR ($CDCl_3$): δ 168.0, 147.7, 137.5, 104.3, 103.9, 42.2, 25.7, 23.9, 23.8, 23.0, 22.49, 22.46, 9.5. Anal. Calcd for $C_{38}H_{77}N_3O_{13}Si_8$: C, 45.25; H, 7.69; N, 4.16. Found: C, 45.13; H, 7.69, N, 4.08.

2.3. Preparation of Poly(amic acid) Precursor to PMDA/ODA (Kapton-like) Polyimide. Polymerizations were carried out in an N_2 filled drybox by the following general procedure: A 50 mL RB-flask was charged with ODA (0.918 g, 4.59 mmol) and DMAc (2 mL). A separate 25 ml RB flask was charged with PMDA (1.000 g, 4.59 mmol) and DMAc (1 mL) to form a light yellow slurry. The latter slurry was added drop-wise to the ODA solution with stirring. Additional DMAc (2 mL aliquots) was added to the PMDA flask to complete transfer to the ODA reaction flask. This was continued until the process was carried out several times with a grand total of 20 mL DMAc for the polymerization reaction. The addition of PMDA to ODA typically took a period of 30 min. The poly(amic acid) solution became highly viscous and was allowed to react for a period of 16 h with stirring at ambient temperature. The poly(amic acid) DMAc solution was stored under nitrogen in a freezer and has been found to produce high-quality films after 5 years of storage.

2.4. Preparation of Poly(amic acid) Precursor to SC POSS/PMDA/ODA Copolymer. In a glovebox, a 25 mL RB-flask was charged with POSS monomer **2** (0.3749 g, 0.3719 mmol), a stir bar, and DMAc (2 mL), and the mixture allowed to stir until homogeneous. A second 50 mL RB-flask was charged with ODA (0.8437 g, 4.21 mmol) and a stir bar. The POSS/DMAc solution was transferred by syringe into the ODA and was stirred. PMDA (1.00 g, 4.59 mmol) was weighed into a 25 ml RB-flask and transferred drop-wise by syringe, as a slurry in DMAc, into the diamine mixture over 30 min. A total of 20 mL of DMAc was added to the polymer solution. The POSS-poly(amic acid) solution became moderately viscous and was stirred overnight at room temperature. The POSS-poly(amic acid) was stored under nitrogen in a freezer, and this solution has been found to produce high-quality films after at least 1 year of storage. This storage time is a conservative estimate because of the limited history of SC-POSS. Comparative main chain POSS-poly(amic acids) have produced high-quality films after at least 5 years of storage under similar conditions, and it is possible that other POSS monomers will behave similarly.

2.5. Fabrication of Free-Standing Polyimide Films. The poly(amic acid) solution, or POSS poly(amic acid) solution, with approximately 2 wt % solids, was poured on a clean glass plate which was balanced in a vacuum oven, equipped with a N_2 flow. The DMAc solvent was evaporated at 80 °C for 4 h, followed by a cure schedule of 120 °C for 1 h, 200 °C for 1 h, and 275 °C for 2 h. The amber colored and visibly transparent films were removed from the slide by placing them under running deioinized water, lifting the film corner with a razor blade, and running water between the glass and the film. The films were stored in air. Side-chain (SC) POSS polyimide films (see Figure 3) were prepared with various percentages of Si_8O_{12} cage, similar to the Si_8O_{11} cage loadings for the MC POSS polyimides described above. Physical properties of the polyimide films are reported elsewhere,[48,49] and they are consistent with complete cure to the Kapton-like polyimide structure (as depicted in Figures 1 and 3). Briefly, the incorporation of POSS increases the coefficient of thermal expansion by about 15% as the weight percentage of the Si_8O_{11}(MC) or Si_8O_{12}(SC) cage goes from 0 to 8.8 wt %, whereas the glass transition temperature decreases by about 10% over this range of POSS loadings. Except for cage loadings above 10 wt %, POSS dispersion has been shown to be fairly uniform, resulting in transparent films with the amber color of PMDA/ODA polyimide. With a cage loading of 7 wt % Si_8O_{11}, the rms surface roughness increases ~20% over that of the pure polyimide.[42]

2.6. Spin-Coated Polyimide and POSS Polyimide Films. Pure polyimide films were prepared from a commercially available poly(amic acid) that has the same chemical repeat unit as DuPont Kapton H (HD MicroSystems PI-5878G), whereas POSS polyimide films were prepared from the MC or SC poly(amic acids) discussed above. Substrates used in the laboratory were 5 MHz sensor crystals (Inficon Maxtek SC-150) for a QCM (Inficon Maxtek RCQM and associated front-load crystal holder). Additional substrates used for LEO flight experiments were quartz discs from quartz crystal oscillators used in electronic circuits (see section 2.7). An adhesion promoter (HD MicroSystems VM-651) was used in the preparation of all spin-coated films. In general, dilution of the poly(amic acid) and spin-coating conditions were adjusted by trial and error to produce cured polyimide films with uniform thicknesses in the range of 1−3 μm (measured with a DekTak^3 surface profiler). A typical spin-coating procedure involves the following steps. (1) Dilute 0.1 mL of

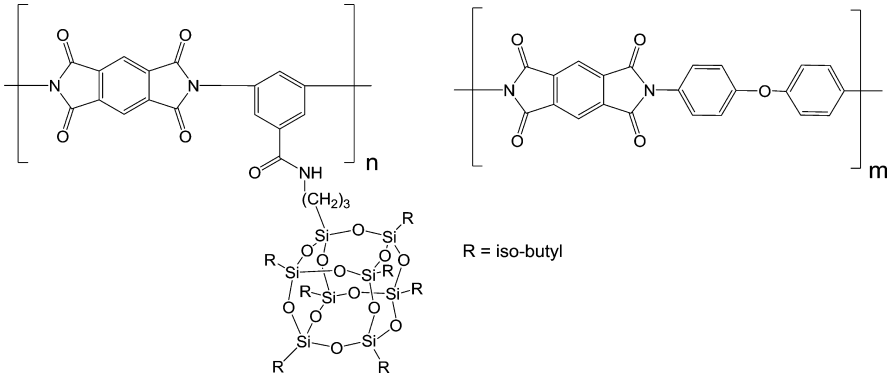

Figure 3. SC POSS polyimide structure demonstrating the PMDA-SC-POSS repeat unit and the PMDA-ODA repeat unit, where R = *iso*-butyl and *n* and *m* are mole fractions that sum to one.

promoter with 120 mL of deionized water. (2) Apply promoter solution to the static QCM disc and let sit for 60 s. (3) Spin at 3000 rpm for 30 s. (4) Bake the promoter-coated disc in an oven at 60 °C for 1.5 h, remove from heat, and allow to cool to room temperature. (5) Apply a few drops of poly(amic acid) solution to completely cover the static disc. (6) Spin at 500 rpm for 10 s. (7) Spin at 5000 rpm for 30 s. (8) Cover the coated disc with a watch glass, allowing a small gap for escape of gas, and let sit for 2 days to allow the solvent to evaporate. (9) Cure coated disc in a temperature-programmable vacuum oven (<100 mTorr) using the following heating program (all heating rates are 1 °C/min): heat to 50 °C and hold for 2 h; heat to 80 °C and hold for 2 h; heat to 200 °C and hold for 1 h; heat to 275 °C and hold for 3 h; cool to 50 °C; turn off heat and allow to cool to room temperature. (10) Remove from vacuum and store in air.

2.7. Low-Earth-Orbit Exposure of POSS Polyimides. POSS polyimide films were exposed to atomic oxygen in the space environment on the Materials International Space Station Experiment (MISSE) platform.[2,54] The atomic-oxygen flux and fluence varied from experiment to experiment, depending on such details as exposure duration, timing of the experiment within the solar cycle, and orientation of MISSE sample tray. The relative velocity of the atomic oxygen with respect to ram surfaces is approximately 7.4 km s^{-1},[55] corresponding to O atoms (in the ground ^3P state) striking the surfaces with an average velocity of 4.5 eV.[56] MC POSS polyimide films were solution coated on aluminum substrates (similar to the procedure described in section 2.5, but without separating the film from the substrate) and flown in LEO on MISSE-1. This flight experiment was retrieved after 3.9 years. The samples were exposed to the ram and therefore all components of the LEO environment, including atomic oxygen and vacuum ultraviolet light, with the O-atom fluence being ~8×10^{21} atoms cm^{-2}, similar to the fluence on the companion MISSE-2 where the fluence was accurately measured to be 8.43×10^{21} atoms cm^{-2}.[2] Free standing films of MC POSS polyimide were sewn to a Kapton blanket and exposed to a sweeping ram (a variety of incidence angles) in LEO on MISSE-5 for about one year. The atomic-oxygen fluence was estimated to be 1.8×10^{20} atoms cm^{-2}. Free-standing films of both MC and SC POSS polyimide films were exposed to the LEO environment in the ram direction on MISSE-6, with a total atomic-oxygen fluence of 1.97×10^{21} atoms cm^{-2}.[57] The step-height difference between the unexposed sample area and the neighboring exposed sample area was measured by a DekTak^3 surface profiler, using the averages of many different step-height measurements. In some cases, the atomic composition of sample surfaces was determined by X-ray photoelectron spectroscopy (XPS). Additional samples of SC POSS polyimides were prepared by spin-coating films of different POSS content onto quartz discs from quartz crystal oscillator modules used for electronic circuits (Abracon 10 MHz). The tops of the quartz crystal oscillator modules were removed with a Dremel tool, and the quartz discs were removed with a razor blade. After the discs were coated with the polyimide, they were inserted back into their respective modules with the use of a conducting adhesive containing silver. The quartz crystal oscillator modules were used in conjunction with an electronic circuit designed and built by Boeing to enable the oscillator to function as a quartz crystal microbalance. The oscillation frequency was converted to a voltage which could be recorded. These QCM samples were exposed on MISSE-6 and the voltage output was recorded on data loggers during flight. The voltage readings were converted to mass loss as a function of time using calibration curves for each sample that were provided by Boeing personnel. A photograph of a post-flight package containing four polyimide-coated crystals may be seen in Figure 4.

2.8. Laboratory Exposure of POSS Polyimides to Atomic Oxygen. Ground-based atomic-oxygen exposures of POSS polyimide samples were performed with a pulsed beam, operating at a repetition rate of 2 Hz and containing O atoms that were generated by the laser-induced breakdown of O_2 gas in a conical nozzle with the use of a 7-joule-per-pulse CO_2 laser.[7,42,58,59] The hyperthermal beam contains neutral O atoms and molecular oxygen, with an ionic component of <0.01%. The mole fraction of atomic oxygen in the beam was above 70%, and for some exposures, above 90%. Kinetic energies of the fast O atoms in the beam averaged 5.2 eV, with a full width at half maximum in the distribution of ~1.5 eV. For some studies, samples were covered with a stainless steel mesh, in order to mask areas and achieve both atomic oxygen exposed and unexposed areas for step-height measurements. For other studies, samples POSS polyimide and control (no-POSS) polyimide films were spin-cast onto quartz crystal microbalance discs, described in Section 2.6, allowing the mass loss of the samples to be measured in situ during an exposure.[59,60] All samples were handled in ambient air after exposure and prior to surface analysis, including erosion depth determination (by profilometry with a DekTak^3 surface profiler) and other surface topography (scanning electron microscopy, SEM) and chemistry (XPS) measurements.

3. RESULTS AND DISCUSSION

3.1. Laboratory Studies of POSS Polyimide Erosion. A detailed laboratory study that included the erosion behavior of MC POSS polyimides at different O-atom fluences was reported earlier,[42] and the results will not be presented here. For comparison with the results reported here, the "10 wt %" and "20 wt %" monomer MC POSS polyimides used in the earlier study are identical to the 3.5 and 7 wt % Si_8O_{11} cage MC POSS polyimides that are discussed in this paper. A key result of the earlier study is that the MC POSS polyimide materials form a passivating silica layer when exposed to atomic oxygen, and this layer grows with time and becomes increasingly resistant to atomic oxygen attack.

A series of SC POSS polyimides was exposed to atomic oxygen in the laboratory at room temperature, with a total fluence near 2.7×10^{20} O atoms cm^{-2}. The results, shown in Table 1, indicate dramatic decreases in surface erosion with increasing content of SC POSS. SC POSS polyimide and MC POSS polyimide had comparable atomic-oxygen erosion yields

Figure 4. Photograph of quartz crystal microbalance flight package that was exposed to the low-Earth-orbital environment on MISSE-6 (PEC-B, ram direction). Four quartz crystals, each with a diameter of 8 mm, may be seen. During the exposure, an aperture of ~6 mm diameter limited the exposed region to the central portion of each disc. Clockwise from upper left: 0 wt % Si_8O_{12} SC POSS polyimide, 7 wt % Si_8O_{12} SC POSS polyimide, 20 wt % Si_8O_{12} SC POSS polyimide, and fluoropolymer (part of an unrelated experiment). The polyimide films were roughly 2 μm thick. Close inspection indicates that the 0 wt % POSS polyimide was eroded away completely in the exposed region, while the POSS-containing films were not eroded away.

Table 1. Laboratory Atomic-Oxygen Erosion Data for SC POSS Polyimides (Adapted with permission from ref 48. Copyright 2009, American Institute of Physics.)

wt % Si_8O_{12} in SC POSS polyimide	Kapton-equivalent fluence ($\times 10^{20}$ O atoms cm^{-2})	erosion depth (μm)	% erosion of Kapton H reference sample
1.75	2.71	1.99 ± 0.01	24.5
3.5	2.66	1.29 ± 0.05	16.15
7.0	2.68	0.390 ± 0.04	4.9
8.8	2.68	0.132 ± 0.02	1.64
10.5	2.71	0.249 ± 0.03	3.06
12.3	2.71	0.113 ± 0.03	1.39
14.0	2.71	Undetectable	~0

(not shown in Table 1). More specifically, in an atomic-oxygen exposure with a total fluence of 3.53×10^{20} O atoms cm^{-2}, 7 wt % Si_8O_{12} SC POSS polyimide had an erosion yield that was 3.3% that of Kapton H. In a separate atomic-oxygen exposure (also at room temperature) with a total fluence of 4.10×10^{20} O atoms cm^{-2}, 7 wt % Si_8O_{11} MC POSS polyimide had an erosion yield that was 3.8% that of Kapton H. The MC and SC POSS polyimides were also exposed side by side to 2.68×10^{20} O atoms cm^{-2}. The percent erosion values of the POSS polyimides relative to Kapton H were 4.25 ± 0.48% for 7 wt % Si_8O_{11} MC POSS polyimide and 4.86 ± 0.47% for 7 wt % Si_8O_{12} SC POSS polyimide. The laboratory-scale synthesis of the polymer films is likely to produce slight differences in molecular weights and cure cycles, thus potentially having minor effects on the atomic-oxygen erosion of the materials. Furthermore, the POSS cage in the SC POSS polyimide has a Si:O ratio of 8:12, whereas the MC POSS polyimide has a Si:O ratio of 8:11. The effect of this slight difference in the POSS cages on the erosion yield is unknown. Nevertheless, the existing data indicate that the atomic-oxygen-induced erosion yields of MC POSS polyimide and SC POSS polyimide are comparable for a given wt % POSS cage. Thus, the level of erosion resistance afforded by POSS appears to depend on the wt % of the POSS cage and not how it is bound to the polymer chain.

The results of a study of the effect of temperature on the atomic-oxygen erosion yield of MC POSS polyimides are summarized in Tables 2 and 3. This study used 0, 3.5, and 7 wt % Si_8O_{11} MC POSS polymide samples that were exposed to the hyperthermal O-atom beam while being held at 25, 100, 150, 220, and 300 °C. Each sample set, corresponding to a particular temperature, was exposed to 50,000 pulses of the hyperthermal O-atom beam. The polyimide sample films were bonded to thermally conducting substrates to ensure temperature equilibration, and each sample set was accompanied by a Kapton H reference sample that was held at 23 °C.[58]

The results in Table 2 show that pure polyimide and MC POSS polyimides experience increasing erosion with increasing temperature. For each temperature, the erosion depths of the MC POSS (Table 2) divided by the erosion depth of Kapton H are given in Table 3. The erosion of the 0 wt % MC POSS polyimide control exhibited the strongest temperature dependence, with the erosion depth increasing by a factor of about 3.6 from 25 to 300 °C. The 3.5 and 7.0 wt % Si_8O_{11} MC POSS polyimides showed less temperature dependence in their erosion. The erosion depths of these samples increased by factors of 2.2 and 2.4, respectively, with the increase in temperature from 25 °C to 300 °C; within the uncertainty in

Table 2. Laboratory Erosion Depths for 0, 3.5, and 7 wt % Si_8O_{11} MC POSS Polyimides after Exposure to Atomic Oxygen at Five Temperatures[a] (Adapted with permission from ref 46. Copyright 2008 American Chemical Society.)

sample temperature (°C)	0 wt % MC POSS polyimide (μm)	3.5 wt % Si_8O_{11} MC POSS polyimide (μm)	7 wt % Si_8O_{11} MC POSS polyimide (μm)	Kapton H 23 °C ref (μm)
300	10.37 ± 0.47	1.24 ± 0.17	0.67 ± 0.16	3.14 ± 0.13
220	7.47 ± 0.37	0.94 ± 0.21	0.78 ± 0.08	3.46 ± 0.20
150	5.36 ± 0.23	1.02 ± 0.11	0.41 ± 0.07	3.59 ± 0.11
100	4.09 ± 0.38	0.82 ± 0.07	0.43 ± 0.06	3.55 ± 0.11
25	3.17 ± 0.24	0.63 ± 0.08	0.30 ± 0.08	3.50 ± 0.12

[a]A Kapton H reference material, held at 23 °C, accompanied each exposure.

Table 3. Ratio of Erosion Depths of 0, 3.5, and 7 wt % Si_8O_{11} MC POSS Polyimides to Erosion Depth of Kapton H Reference Material, Held at 23 °C (Adapted with permission from ref 46. Copyright 2008 American Chemical Society.)

sample temperature (°C)	0 wt % MC POSS polyimide/ Kapton H	3.5 wt % Si_8O_{11} MC POSS polyimide/ Kapton H	7 wt % Si_8O_{11} MC POSS polyimide/ Kapton H
300	3.3 ± 0.20	0.40 ± 0.06	0.21 ± 0.05
220	2.16 ± 0.16	0.27 ± 0.06	0.23 ± 0.03
150	1.49 ± 0.08	0.28 ± 0.03	0.11 ± 0.02
100	1.15 ± 0.11	0.23 ± 0.02	0.12 ± 0.02
25	0.91 ± 0.08	0.18 ± 0.02	0.086 ± 0.02

the measurements, these factors may be considered to be the same.

The results demonstrate that although MC POSS polyimides have increased erosion yields with increasing temperature, they certainly erode less than the 0 wt % MC POSS control at elevated temperatures. In most cases, except at 220 °C, a doubling of the POSS content from 3.5 to 7.0 wt % Si_8O_{11}, causes the erosion depth to decrease by about half. The O-atom fluences used in this study are relatively low. It has been seen that with higher O-atom fluences, at room temperature, there is an increasing difference in the erosion of pure polyimide and POSS polyimide (see ref 42 and new results below). This is because the erosion of polyimide increases linearly with fluence while the erosion of POSS polyimide decreases exponentially with fluence. Hence, it is expected that higher fluence exposures at elevated temperatures may reveal a more marked reduction in the erosion yields for POSS polyimides compared to the erosion yields for the 0 wt % POSS polyimide and Kapton H polymers. A mechanistic reason for the apparent enhancement in the durability of MC POSS polyimide relative to Kapton H at elevated temperatures is not known. Perhaps the higher temperature helps speed the formation of a SiO_x passivation layer.

A "self-passivation test" was carried out to demonstrate that a POSS polyimide can maintain a low erosion yield even if its initial passivation layer becomes damaged. Multiple samples of Kapton H, 8.8 wt % Si_8O_{11} MC POSS polyimide, and silica-coated Kapton HN (provided by Astral Technology Unlimited, Inc., Lot No. 00625-007), with a 130 nm SiO_2 coating) were exposed successively to the hyperthermal atomic-oxygen beam. Initially, one sample of each material was covered by a screen, to provide exposed and protected areas for erosion depth measurements. The samples were exposed and removed from the chamber. The erosion depths of the screened samples were then measured. Another set of samples was scratched. For each sample, one scratch, approximately 40 μm wide and 1 μm deep, was made with a diamond-tipped scribe, and two scratches, approximately 20 μm wide and 1 μm deep, were made with a razor blade. All scratches were measured by profilometry (with a 5 μm radius probe tip) in several places. Screens were placed over the scratched samples and these samples were exposed to a similar O-atom fluence from the hyperthermal atomic-oxygen beam. After removal of the samples from the chamber, profilometry was used to measure step-height differences between exposed and unexposed areas and to profile each scratch in the exposed and unexposed regions.

The erosion depths for each condition are summarized in Table 4. The erosion depth of the Kapton H sample after the initial exposure was 7.0 ± 0.2 μm, indicating an O-atom fluence of 2.3×10^{20} O atoms cm^{-2}. This sample appeared to be significantly roughened after exposure, as is typically observed.[3,7] The erosion depth of 0.26 ± 0.15 μm for the 8.8 wt % Si_8O_{11} MC POSS polyimide film was difficult to measure, as the overall etch depth was not much greater than the slight roughness caused by the exposure. For the SiO_2-coated Kapton HN sample, the erosion depth was below the measurement limit of the surface profiler and the sample surface appeared to be unaffected when viewed through a light microscope.

Table 4. Erosion Depths for Three Materials That Were Exposed to Atomic Oxygen, Scratched, Then Exposed Again[a] (Adapted with permission from ref 46. Copyright 2008 American Chemical Society.)

	Kapton H (μm)	SiO_2-coated Kapton HN (μm)	8.8 wt % Si_8O_{11} MC POSS polyimide (μm)
erosion depth after 1st exposure	7.0 ± 0.20	~0	0.26 ± 0.15
erosion depth outside of scratch after 2nd exposure	5.45 ± 0.55	~0	~0
erosion depth inside of scratch after 2nd exposure	6.02 ± 0.60	6.34 ± 0.54	0.15 ± 0.18

[a]The SiO_2 coating on the second sample was 130 nm thick.

SEM images of Kapton H, SiO_2-coated Kapton HN, and 8.8 wt % Si_8O_{11} MC POSS polyimide that were exposed, scratched, and exposed again are shown in Figure 5. For the SEM image of Kapton H, the exposed region is on the left side of the image and has a more roughened surface with a deepened scratched area. The erosion depth of the Kapton H sample outside of the scratch was about 5.5 μm. The unexposed scratch was ~20 μm wide and ~1 μm deep and became ~1.5 μm deep relative to the neighboring eroded surface after the second exposure. Thus, the erosion depth of Kapton H inside the scratch was ~6 μm. The top region of the SiO_2-coated Kapton HN image was exposed and only had erosion in the scratched area, while the neighboring SiO_2-coated Kapton

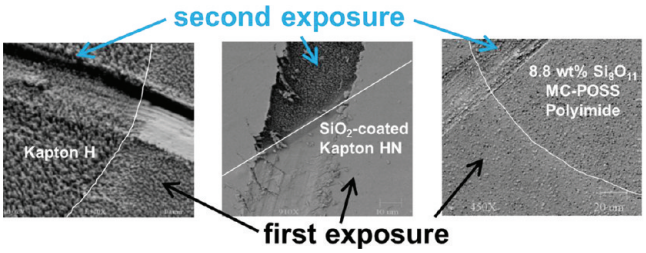

Figure 5. SEM images of three samples that were exposed to atomic oxygen, scratched, covered with an etched stainless-steel mesh, then exposed again. These images were obtained after the second exposure. The white lines on the images indicate dividing lines between the regions that were protected underneath stainless steel portions of the mesh ("first exposure") and the regions that were unprotected by the mesh ("second exposure"). The SiO_2 coating on the second sample was 130 nm thick.

HN remained unaffected, demonstrating the effects of damage to silica coatings on Kapton. Here the unexposed scratch was ~20 μm wide and ~1 μm deep and the exposed scratch was ~7.3 μm deep relative to the neighboring exposed surface, amounting to ~6.3 μm of erosion in the scratch. 8.8 wt % Si_8O_{11} MC POSS polyimide was exposed in the darkened upper right area in Figure 5. It is very difficult to discern the difference in the scratches in the covered ("first exposure") and uncovered ("second exposure") regions. The erosion depth of the unscratched region resulting from the second exposure was immeasurably small. The average difference in erosion depth between covered and uncovered scratches is ~0.15 μm, which is approximately how much this MC POSS polyimide would be expected to erode after this exposure. One may conclude from this result that even though any passivating layer would have been removed by the scratch, the underlying POSS-containing material must have re-formed a passivating layer in the region of the scratch and therefore only eroded a tiny amount (~0.15 μm). The Kapton H and SiO_2-coated Kapton HN samples eroded slightly deeper inside their scratches than was expected based on the erosion depth of the Kapton H outside the scratch. The slight increase in erosion depth inside the scratch vs. outside the scratch might be explained by enhanced erosion inside the scratch resulting from the focusing of incoming O atoms through forward scattering from the sidewalls of the scratches.[61] This effect would not be expected to be as significant for the MC POSS polyimide, because the scratched region never becomes very deep.

3.2. Erosion of POSS Polyimides on the International Space Station. MC POSS polyimide films with 0, 1.75, and 3.5 wt % were flown on MISSE-1. Various images of the samples were taken throughout the flight, and these show that the 0 wt % MC POSS polyimide control sample was completely eroded in less than four months. Photographs of the samples that were returned to Earth after the mission are shown in Figure 6. The 0 wt % sample was completely eroded away, leaving the bare aluminum substrate. The 1.75 wt % sample had some remaining film, and the 3.5 wt % sample was largely intact. The step heights between the uneroded regions of each sample (the circular regions under a clamping ring) and the eroded regions are shown in Table 5. The step height of the 0 wt % POSS polyimide was 32.6 ± 0.9 μm, indicating that this was the original film thickness (because the exposed film was completely eroded away). On the basis the estimated O-atom fluence of ~8×10^{21} atoms cm^{-2} and an erosion yield

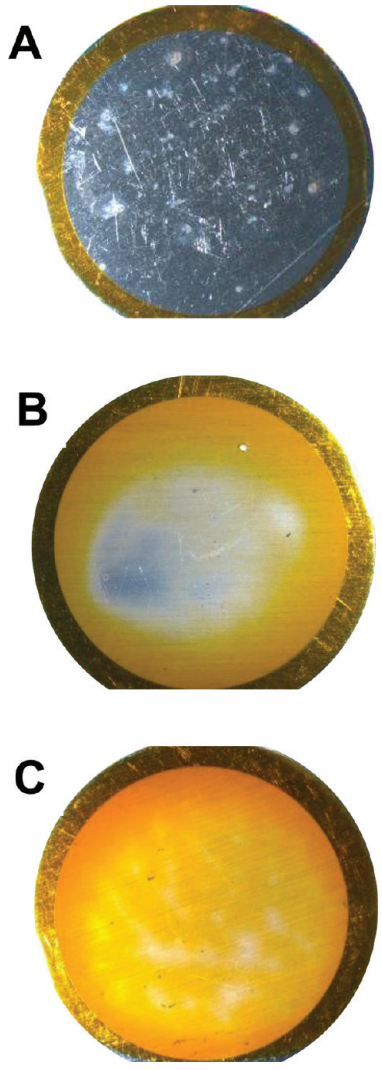

Figure 6. From top to bottom: 0, 1.75, and 3.5 wt % Si_8O_{11} MC POSS polyimides that were exposed to the LEO environment for 3.9 years on MISSE-1. The outer ring of material was not exposed to the space environment.

of 3.00×10^{-24} cm^3 $atom^{-1}$ for Kapton H,[58] the 0 wt % polyimide should have eroded a minimum of 240 μm. This value is a minimum, because the O-atom fluence estimate is probably too low and because the erosion yield of the laboratory-prepared pure polyimide is likely to be higher than that of Kapton H by 10–20% (see Tables 6 and 7 and relevant discussion). Thus, the two 1.75 and 3.5 wt % POSS polyimides had erosion yields that were only about 0.06 and 0.02, respectively, that of Kapton H and perhaps as little as 0.02 and

Table 5. MISSE-1 Flight MC-POSS Polyimide Erosion Data (Adapted with permission from ref 48. Copyright 2009 American Institute of Physics.)

sample	erosion depth (μm)	erosion on ISS in 3.9 years (μm)
0 wt % Si_8O_{11} MC POSS polyimide	32.6 ± 0.9 (original film thickness)	240-290 (240 μm for Kapton H)
1.75 wt % Si_8O_{11} MC POSS polyimide	5.8 ± 1.3	5.8
3.5 wt % Si_8O_{11} MC POSS polyimide	2.1 ± 0.3	2.1

dx.doi.org/10.1021/am201509n | ACS Appl. Mater. Interfaces 2012, 4, 492–502

Table 6. MISSE-5 Flight MC POSS Polyimide Erosion Data (Adapted with permission from ref 48. Copyright 2009 American Institute of Physics.)

sample	erosion depth (μm)
Kapton H	2.42 ± 0.47
0 wt % POSS polyimide	2.89 ± 0.59
1.75 wt % Si_8O_{11} MC-POSS polyimide	1.15 ± 0.21
3.5 wt % Si_8O_{11} MC-POSS polyimide	0.44 ± 0.19
5.3 wt % Si_8O_{11} MC-POSS Polyimide	0.31 ± 0.18
7.0 wt % Si_8O_{11} MC-POSS polyimide	0.25 ± 0.11

Table 7. MISSE-6 Flight POSS Polyimide Erosion Data

sample	erosion depth (μm)
Kapton H	59.1 ± 1.5[a]
0 wt % POSS polyimide	75.9 ± 4.2
7 wt % Si_8O_{12} SC-POSS polyimide	1.37 ± 0.22
7 wt % Si_8O_{11} MC-POSS polyimide	1.02 ± 0.30
8.8 wt % Si_8O_{12} SC-POSS polyimide	0.44 ± 0.16
8.8 wt % Si_8O_{11} MC-POSS polyimide	0.74 ± 0.22

[a]From ref 57.

0.007, respectively, that of the 0 wt % POSS polyimide control material. It was determined by XPS that the atomic percentages were 34% Si, 59% O, and 7% C for of the top ~10 nm of both the 1.75 and 3.5 wt % Si_8O_{11} MC POSS polyimide samples. The XPS data are therefore consistent with the formation of a passivating silica (SiO_2) layer on the POSS polyimides. SEM images of the 1.75 and 3.5 wt % Si_8O_{11} MC POSS polyimides (Figure 7) show less roughness on the sample with the higher POSS content, suggesting that the passivation layer is more connected on this surface. These eroded surfaces may be compared with those from laboratory exposures,[42] where it is seen that the roughness of the eroded MC POSS polyimide surfaces is much less than that of the 0 wt % POSS polyimide control.

Several MC POSS polyimides, with 0, 1.75, 3.5, 5.25, and 7.0 wt % Si_8O_{11}, were flown on MISSE-5 and experienced an approximate fluence of 1.8×10^{20} atoms cm^{-2}. These samples were located on the top side of the International Space Station and, although they were exposed to all components of the LEO environment, they were situated such that a part of the ISS obstructed the ram and therefore reduced the atomic-oxygen fluence and made the incidence angle ill-defined. The erosion depths decreased with increasing POSS content, as shown in Table 6. The 0 wt % POSS polyimide, which was synthesized by the same technique as the POSS-containing polyimides, eroded ~20% more than commercial Kapton H. The difference between the erosion depths of the POSS-containing samples and that of Kapton H is significantly less than what was inferred for the MISSE-1 samples. The relative O-atom resistance of POSS-containing polyimides is expected to increase with longer exposures. During the initial stages of oxidation of a POSS polyimide, erosion of the organic component occurs and will compete with the development of a SiO_2 passivation layer. Therefore, during long exposures, such as MISSE-1, POSS-containing polyimides will form a steady-state passivation layer and reach their minimum reactivity, whereas a pure polyimide will continue to erode at a constant rate. On the basis of earlier laboratory experiments,[42] we would conclude that the passivation layer had not fully formed by the end of the MISSE-5 mission, so the erosion rate of the POSS-containing samples relative to that of Kapton H would not have reached its minimum level.

MC and SC POSS polyimide samples were exposed to atomic oxygen in the ram direction on MISSE-6 (Tray 6A). The estimated O-atom fluence, based on the etch depth of a Kapton H standard material, was fairly high at 1.97×10^{21} atoms cm^{-2}. The step heights for pure polyimide and polyimides with 7 wt % and 8.8 wt % SC POSS and 7 wt % and 8.8 wt % MC POSS are shown in Table 7. The pure polyimide has an erosion depth (75.9 μm) that is roughly 20% higher than the erosion depth (59 μm) of the commercial polyimide, Kapton H. This result is consistent with the erosion difference between Kapton H and 0 wt % POSS polyimide on MISSE-5 (seeTable 6). Apparently,the erosion yields of these two polyimides are different, even though they share the same chemical repeat unit in their polymer backbones. The 0 wt % POSS control material is prepared in the laboratory and is presumably more pure than Kapton H. Perhaps residual impurities from the industrial processing of Kapton H reduce the erosion yield slightly with respect to the pure polyimide, or perhaps the molecular weight of the lab-prepared polyimide is lower. The SC and MC POSS polyimides that were exposed on MISSE-6 have much lower erosion depths than the 0 wt % POSS polyimide or Kapton H samples. The uncertainties represent $\pm 1\sigma$ in the series of measurements for each sample; however,

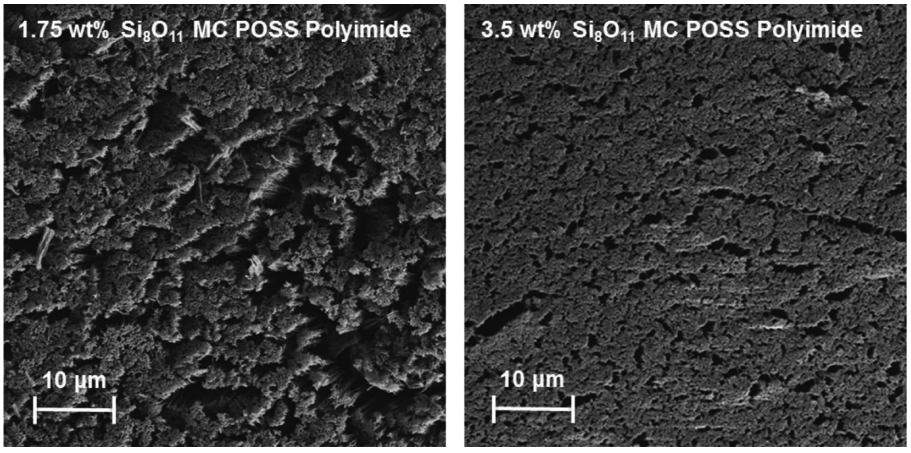

Figure 7. Scanning electron microscope images of two MC POSS polyimides that were exposed to the LEO environment for 3.9 years on MISSE-1. The magnification in both images is 1370.

the true uncertainty is probably larger, because the POSS-containing samples were somewhat rough, making the small step heights difficult to measure precisely. Nevertheless, it is clear that the higher POSS cage content tended to decrease the erosion depth, and the MC and SC POSS polyimides behaved similarly. These results are consistent with what was observed for the samples exposed on MISSE-1, given the potential uncertainties in the measurements and different mission profiles. In both cases, the incorporation of POSS into the polyimide can reduce the erosion yield to less than 2% that of Kapton H.

3.3. In situ Studies of POSS Polyimide Erosion Kinetics with QCMs. Several SC POSS polyimide films were spin-coated onto quartz crystal discs and exposed on MISSE-6, and their mass losses were measured in situ with QCMs (see Fig. 8).

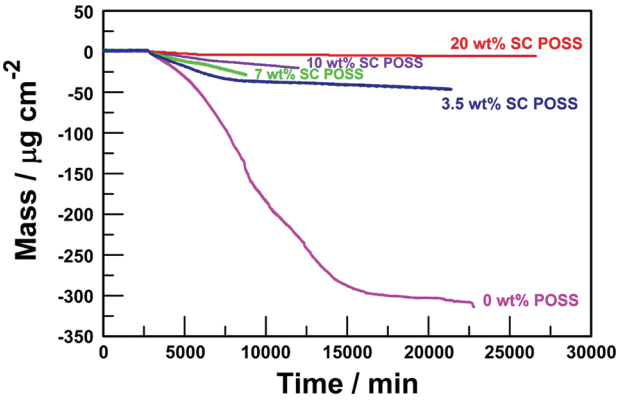

Figure 8. Mass loss, measured by quartz crystal microbalances, of various SC POSS polyimide films as a function of exposure duration on the MISSE-6 space flight experiment. The labels refer to the weight percent Si_8O_{12} SC POSS in the polyimide samples. The mass loss rate for the 0 wt % POSS polyimide is constant until the material is eroded away, at which point the mass loss rate appears to go to zero.

Although all QCMs failed long before the end of the mission (apparently because of the oxidation of silver electrical contacts, or perhaps other components) and the temperature of the QCMs was not carefully controlled, it is clear from the data that were collected that POSS-containing polyimides suffered significantly less mass loss than a 0 wt % POSS polyimide control. Although the data were somewhat uncertain, the mass loss rate appears to be relatively high initially on the POSS polyimide samples and then to decrease with exposure duration. In contrast, the 0 wt % POSS polyimide control loses mass at a roughly constant rate of 0.0297 μg cm^{-2} min^{-1}, regardless of the exposure duration, until the sample has been essentially eroded away. This mass loss rate provides a rough estimate of the O-atom flux during the early part of the MISSE-6 mission of $\sim 1 \times 10^{14}$ O atoms cm^{-2} s^{-1}, assuming a density of 1.42 g cm^{-3} and an erosion yield of 3.3×10^{-24} for the polyimide. These assumed values are both subject to uncertainties of at least $\pm$10%.

Laboratory measurements of mass loss with QCM samples yielded much more precise data than what was collected with the MISSE-6 experiment. Figure 9 shows mass loss as a function of exposure duration in the hyperthermal beam for two MC POSS polyimides, one SC POSS polyimide, and a 0 wt % POSS polyimide control. Similar to the MISSE-6 results, these results demonstrate that the mass loss rate of POSS-containing polyimides decreases with exposure duration and that higher POSS content leads to lower mass loss rate. The similar mass loss rates for 7 wt % Si_8O_{12} SC POSS polyimide

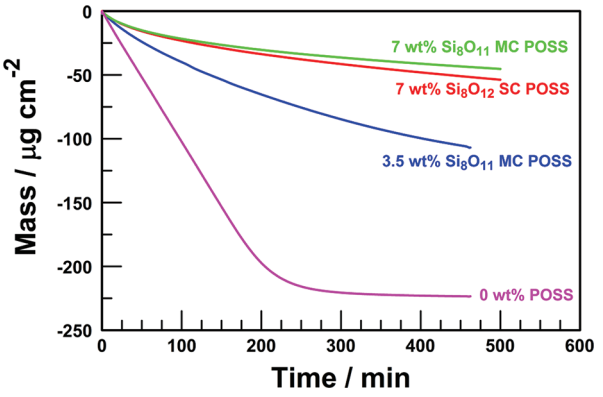

Figure 9. Mass loss of various POSS polyimides as a function of exposure to a hyperthermal atomic-oxygen beam in the laboratory. The mass loss rate for the 0 wt % POSS polyimide is constant until the material is eroded away, at which point the mass loss rate appears to go to zero. The mass loss rates of the POSS-containing samples are much less than the 0 wt % POSS polyimide control, and their mass loss rates decrease with time and appear to tend toward, but do not reach, a constant low value.

and 7 wt % Si_8O_{11} MC POSS polyimide are consistent with the erosion data, which indicate that the wt% of POSS and not the way in which the POSS cage is bound to the polymer backbone, determines the level of atomic-oxygen protection afforded to a polyimide by POSS. The observation of a decreasing mass loss rate for the POSS polyimides and a constant mass loss rate for the polyimide control is further evidence for the formation of a passivation layer as the POSS polyimides are exposed to atomic oxygen. Apparently, the exposures were not long enough in these experiments to make the mass loss rate go to zero, or to a constant value. It is possible that the passivation layer never becomes completely impervious to atomic oxygen; thus, the mass loss rate may be ultimately finite, albeit very low. The in situ measurements of the mass loss rates of different POSS polyimides may serve as a basis for theoretical simulations of the erosion mechanisms and the consequent erosion kinetics. At this point, however, predictions of the space durability of POSS polyimides must be based on the aggregate knowledge generated from the empirical studies presented here.

CONCLUSIONS

A large amount of empirical data have been collected on the effects of hyperthermal atomic oxygen on POSS polymides with various weight percentages of POSS cages that are bound to the polymer backbone in main-chain or side-chain configurations. In general, the following conclusions have been reached. During POSS polyimide exposure to atomic oxygen, organic material is degraded and a silica passivation layer is formed. This silica layer protects the underlying polymer from further degradation. Depending on the weight percentage of the POSS cage, the erosion yield of the POSS polyimide may be as little as ~0.01 that of the pure polyimide (or Kapton H). The POSS polyimide surface has been shown to re-grow the passivation layer ("self-heal") if the initial silica layer is scratched. The rate of the decrease in reactivity of the surface with exposure time has been studied by measuring mass loss in real time with a quartz crystal microbalance. It has been found that the resistance of POSS polyimide to O-atom attack depends on the weight percentage of the POSS cage in the polymer rather than on how it is copolymerized with the

dx.doi.org/10.1021/am201509n | ACS Appl. Mater. Interfaces 2012, 4, 492–502

polyimide backbone, suggesting that lower-cost POSS monomers, such as the side-chain monomer studied here, may be pursued for the production of space-durable polyimides. All the results collected in both the laboratory and space experiments are consistent and show the value of laboratory experiments with the laser-detonation source to predict the durability of materials in the actual LEO environment. The aggregated results of all the experiments with POSS polyimides demonstrate great promise for POSS polyimides as drop-in replacements for the ubiquitous spacecraft polymer, Kapton.

AUTHOR INFORMATION

Corresponding Author

*E-mail: tminton@montana.edu.

ACKNOWLEDGMENTS

This work was supported by the Defense Advanced Research Projects Agency (DARPA), the Air Force Office of Scientific Research (Grants F49620-01-1-0276 & LRIR-92PL0COR), and the National Science Foundation (CHE-0943639).

REFERENCES

(1) Dever, J.; Banks, B.; de Groh, K.; Miller, S. Degradation of Spacecraft Materials. In *Handbook of Environmental Degradation of Materials*; Kutz, M., Ed.; William Andrew Publishers: Norwich, NY, 2005; chapter 23, pp 465−502.

(2) de Groh, K. K.; Banks, B. B.; McCarthy, C. E.; Rucker, R. N.; Roberts, L. M.; Berger, L. A. *High Perform. Polym.* **2008**, *20*, 388.

(3) Banks, B. A.; de Groh, K. K.; Miller, S. K. Low Earth Orbital Atomic Oxygen Interactions with Spacecraft Materials; NASA/TM-2004-213400; National Aeronautics and Space Administration: Washington, D.C., 2004.

(4) de Groh, K. K.; Banks, B. A., Techniques for Measuring Low Earth Orbital Atomic Oxygen Erosion of Polymers. In *2002 Symposium and Exhibition Sponsored by the Society for the Advancement of Materials and Process Engineering*; Long Beach, CA, May 12−16, 2002; Society for the Advancement of Materials and Process Engineering: Covina, CA, 2002.

(5) Koontz, S. L.; Leger, L. J.; Visentine, J. T.; Hunton, D. E.; Cross, J. B.; Hakes, C. L. *J. Spacecr. Rockets* **1995**, *32* (3), 483−495.

(6) Banks, B. A.; Rutledge, S. K.; de Groh, K. K.; Mirtich, M. J.; Gebauer, L.; Olle, R.; Hill, C. M. The Implication of the LDEF Results on Space Freedom Power System Materials. In *Proceedings of the 5th International Symposium on Material in a Space Environment*; Cannes-Mandelieu, France, Sept 16−20, 1991; p 137.

(7) Minton, T. K.; Garton, D. J., Dynamics of Atomic-Oxygen-Induced Polymer Degradation in Low-Earth Orbit. In *Advanced Series in Physical Chemistry—11: Chemical Dynamics in Extreme Environments*; Dressler, R. A., Ed.; World Scientific: Singapore, 2001; pp 420−489.

(8) Dooling, D.; Finckenor, M. M. *Material Selection Guidelines to Limit Atomic Oxygen Effects on Spacecraft Surfaces*; NASA/TP-1999-209260; National Aeronautics and Space Administration: Washington, D.C., 1999.

(9) Koontz, S. L.; Leger, L. J.; Rickman, S. L.; Hakes, C. L.; Bui, D. T.; Hunton, D. E.; Cross, J. B. *J. Spacecr. Rockets* **1995**, *32*, 475.

(10) Zhang, J; Minton, T. K. *High Perform. Polym.* **2001**, *13*, S467.

(11) Zhang, J.; Garton, D. J.; Minton, T. K. *J. Chem. Phys.* **2002**, *117*, 6239.

(12) Gindulyte, A.; Massa, L.; Banks, B. A.; Rutledge, S. K. *J. Phys. Chem. A* **2002**, *106*, 5463.

(13) Gindulyte, A.; Massa, L.; Banks, B. A.; Miller, S. K. R., Direct C-C Bond Breaking in the Reaction of $O(^3P)$ in Low Earth Orbit. In *Space Technology Proceedings-5: Protection of Materials and Structures from the Space Environment*; Springer: New York, 2003; pp 299−306.

(14) Troya, D.; Schatz, G. C. *Int. Rev. Phys. Chem.* **2004**, *23*, 341.

(15) Troya, D.; Schatz, G. C. *J. Chem. Phys.* **2004**, *120*, 7696.

(16) Zhang, J.; Upadhyaya, H. P.; Brunsvold, A. L.; Minton, T. K. *J. Phys. Chem. B* **2006**, *110*, 12500.

(17) Kim, D.; Schatz, G. C. *J. Phys. Chem. A* **2007**, *111*, 5019.

(18) Brunsvold, A. L.; Upadhyaya, H. P.; Zhang, J.; Minton, T. K. *ACS Appl. Mater. Interfaces* **2009**, *1*, 187.

(19) Garton, D. J.; Minton, T. K.; Hu, W.; Schatz, G. C. *J. Phys. Chem. A* **2009**, *113*, 4722.

(20) Tagawa, M.; Minton, T. K. *MRS Bull.* **2010**, *35*, 35.

(21) Champion, K. S. W.; Cole, A. E.; Kantor, A. J. Standard and Reference Atmospheres. In *Handbook of Geophysics and the Space Environment*; Jursa, A. S., Ed.;National Technical Information Service: Springfield, VA, 1985; pp 14−43.

(22) Hedin, A. E. *J. Geophys. Res.−Space Phys.* **1983**, *88* (A12), 170.

(23) Rutledge, S. K.; Mihelcic, J. A., The Effect of Atomic Oxygen on Altered and Coated Kapton Surfaces for Spacecraft Applications in Low Earth Orbit. *Proceedings of a Symposium Sponsored by TMS-ASM Joint Corrosion and Environmental Effects Committee and the 199th Annual Meeting of the Minerals, Metals, and Materials Society*; Anaheim, CA, Feb 17−22, 1990; Minerals, Metals, and Materials Society: Warrendale, PA, 1990.

(24) Rutledge, S. K.; Olle, R. M., Space Station Freedom Solar Array Blanket Coverlay Atomic Oxygen Durability Testing Results. *Proceedings from the 38th International SAMPE Symposium*; Anaheim, CA, May 10−13, 1993 ; Society for the Advancement of Material and Process Engineering: Covina, CA, 1993.

(25) de Groh, K. K.; Banks, B. A. *J. Spacecr. Rockets* **1994**, *31*, 656.

(26) Tennyson, R. C. *Surf. Coat. Technol.* **1994**, *68/69*, 519−527.

(27) Zhang, X.; Wu, Y.; He, S.; Yang, D. *Yuhang Cailiao Gongyi* **2007**, *37*, 19.

(28) Devapal, D.; Packirisamy, S.; Korulla, R. M.; Ninan, K. N. *J. Appl. Polym. Sci.* **2004**, *94*, 2368−2375.

(29) Kleiman, J. I. *MRS Bull.* **2010**, *35*, 55.

(30) Gilman, J. W.; Schlitzer, D. S.; Lichtenhan, J. D. *J. Appl. Polym. Sci.* **1996**, *60*, 591−596.

(31) Gonzalez, R. I.; Phillips, S. H.; Hoflund, G. B. *J. Spacecr. Rockets* **2000**, *37*, 463−467.

(32) Wagner, S.; Dai, H.; Stapleton, R. A.; Illingsworth, M. L.; Siochi, E. J. *High Perform. Polym.* **2006**, *18*, 399−419.

(33) Wang, X.; Zhao, X.; Wang, M.; Shen, Z. *Nucl. Instrum. Methods Phys. Res., Sect. B* **2006**, *243*, 320−324.

(34) Heltzel, S.; Semprimoschnig, C. O. A. *High Perform. Polym.* **2004**, *16*, 235.

(35) Karam, R. D.; Zarchan, P. *Progr. Astronaut. Aeronaut.* **1998**, 181.

(36) Connell, J. W.; Watson, K. A. *High Perform. Polym.* **2001**, *13*, 23.

(37) Verker, R.; Grossman, E.; Gouzman, I.; Eliaz, N. *Polymer* **2007**, *48*, 19.

(38) Musto, P.; Ragosta, G.; Scarinzi, G.; Mascia, L. *Polymer* **2004**, *45*, 4265.

(39) Hergenrother, P. M., Condensation Polyimides. In *Encyclopedia of Composites*; Lee, S. M., Ed.; VCH Publishers: New York, 1990.

(40) Sroog, C. E. *J. Polym. Sci.: Macromol. Rev.* **1976**, *11*, 161.

(41) Gonzalez, R. I. Synthesis and In-Situ Atomic Oxygen Erosion Studies of Space-Survivable Hybrid Organic/Inorganic POSS Polymers. Ph.D. Dissertation, Chemical Engineering Department, University of Florida, Gainesville, FL, 2002; http://purl.fcla.edu/fcla/etd/UFE1000127.

(42) Brunsvold, A. L.; Minton, T. K.; Gouzman, I.; Grossman, E.; Gonzalez, R. I. *High Perform. Polym.* **2004**, *16*, 303.

(43) Phillips, S. H.; Haddad, T. S.; Tomczak, S. J. *Curr. Opin. Solid State Mater. Sci.* **2004**, *8*, 21.

(44) Tomczak, S. J.; Marchant, D.; Svejda, S.; Minton, T. K.; Brunsvold, A. L.; Gouzman, I.; Grossman, E.; Schatz, G. C.; Troya, D.; Sun, L. P.; Gonzalez, R. I. *Mater. Res. Soc. Symp. Proc.* **2005**, *851*, 395.

(45) Tomczak, S. J.; Vij, V.; Marchant, D.; Minton, T. K.; Brunsvold, A. L.; Wright, M. E.; Petteys, B. J.; Guenthner, A. J. *Proc. SPIE* **2006**, *6308*, 630804.

(46) Tomczak, S. J.; Vij, V.; Minton, T. K.; Brunsvold, A. L.; Marchant, D.; Wright, M. E.; Petteys, B. J.; Guenthner, A. J.;

Yandek, G. R.; Mabry. J. M. *Comparisons of Polyhedral Oligomeric Silsesquioxane Polyimides as Space-Survivable Materials*; ACS Symposium Series; American Chemical Society: Washington, D.C., 2008; vol. *978*, pp 140−152.
(47) Tomczak, S. J.; Wright, M. E.; Guenthner, A. J.; Petteys, B. J.; Minton, T. K.; Brunsvold, A.; Vij, V.; McGrath, L. M.; Mabry, J. M. The Effect of Atomic Oxygen on POSS Polyimides. *SAMPE Conference Proceedings 2008*; Society for the Advancement of Materials and Process Engineering: Covina, CA, 2008; Vol. *53*, pp 306/1−306/15.
(48) S. J. Tomczak., M. E. Wright., A. J. Guenthner., B. J. Pettys., A. L. Brunsvold., C. Knight., T. K. Minton., V. Vij., L. M. McGrath., J. M. Mabry. Space Survivability of Main-Chain and Side-Chain POSS-Kapton Polyimides. In *AIP Conference Proceedings: Materials Physics and Applications*; Kleiman, J. I, Ed.; Springer: New York, 2009; Vol. *1087*, pp 505−518.
(49) Tomczak, S. J.; Wright, M. E.; Guenthner, A. J.; Petteys, B. J.; Minton, T. K.; Brunsvold, A.; Vij, V.; McGrath, L. M.; Mabry, J. M. *Polyimides Other High Temp. Polym.* **2009**, *5*, 227−245.
(50) Verker, R.; Grossman, E.; Gouzman, I.; Eliaz, N. *High Perform. Polym.* **2008**, *20*, 475.
(51) Verker, R.; Grossman, E.; Gouzman, I.; Eliaz, N. *Composites Sci. Technol.* **2009**, *69*, 2178.
(52) Verker, R.; Grossman, E.; Eliaz, N. *Acta Mater.* **2009**, *57*, 1112.
(53) Wright, M. E.; Schorzman, D. A.; Feher, F. J.; Jin, R. Z. *Chem. Mater.* **2003**, *15*, 264.
(54) Edwards, D. L.; Tighe, A. P.; Van Eesbeek, M.; Kimoto, Y.; de Groh, K. K. *MRS Bull.* **2010**, *35*, 25.
(55) Murad, E. *J. Spacecr. Rockets* **1996**, *33*, 131.
(56) Banks, B. A.; de Groh, K. K.; Rutledge, S. K.; DiFilippo, F. J., *Prediction of In-Space Durability of Protected Polymers Based on Ground Laboratory Thermal Energy Atomic Oxygen*; NASA Technical Memorandum 107209; National Aeronautics and Space Administration: Washington, D.C., 1996.
(57) de Groh, K. K.; Banks, B. A.; Guo, A.; Ashmead, C. C.; Mitchell, G. G.; Yi, G. T., MISSE-6 Polymers Atomic Oxygen Erosion Data. Presented at the *2010 National Space & Missile Materials Symposium (NSMMS)*; Scottsdale, AZ, June 28−July 1, 2010.
(58) Buczala, D. M.; Brunsvold, A. L.; Minton, T. K. *J. Spacecr. Rockets* **2006**, *43*, 421.
(59) Minton, T. K.; Wu, B.; Zhang, J.; Lindholm, N. F.; Abdulagatov, A. I.; O'Patchen, J.; George, S. M.; Groner, M. D. *ACS Appl. Mater. Interfaces* **2010**, *2*, 2515.
(60) Zhang, J.; Lindholm, N. F.; Brunsvold, A. L.; Upadhyaya, H. P.; Minton, T. K.; Tagawa, M. *ACS Appl. Mater. Interfaces* **2009**, *1*, 653.
(61) Hwang, G. S.; Anderson, C. M.; Gordon, M. J.; Moore, T. A.; Minton, T. K.; Giapis, K. P. *Phys. Rev. Lett.* **1996**, *77*, 3049.